Geant4 Simulations for the Nab experiment:

Electro-Magnetic Spectrometer

L.P. Alonzi III

February 19, 2009

1. Motivation

Precise measurements of fundamental particle decays are a critical component to the progress of human understanding of the universe. It is from the crucible of these measurements that the Standard Model is honed and new physics is discovered. For neutron beta decay these advancements come in the form of knowledge of the ratio G_A/G_V as well as detection of possible deviations from the $V-A$ structure of the weak nuclear force. This knowledge when combined with a measurement of the neutron lifetime has ramifications as far reaching as CKM unitarity and constraints on new physics.

In the zero-recoil approximation neglecting radiative and loop corrections with parameters a and b,

$$\partial\Gamma_n \propto p_e E_e p_\nu E_\nu \left(1 + a\frac{\vec{p}_e \cdot \vec{p}_\nu}{E_e E_\nu} + b\frac{m_e}{E_e} + \vec{\sigma}_n \cdot \vec{f}(\vec{p}_e, \vec{p}_\nu)\right). \tag{1}$$

Where p_e, E_e, p_ν, E_ν, and $\vec{\sigma}_n$ are the electron momentum, electron energy, neutrino momentum, neutrino energy, and neutron spin, respectively [1]. The Nab experiment will use a novel 4π magnetic spectrometer to detect neutron decay products from the Fundamental Neutron Physics Beamline at the Spallation Neutron Source in Oak Ridge, Tennessee.

The spectrometer will be a 4 m long cylindrical cavity with a longitudinal magnetic field. The neutron beam enters the middle of the cavity perpendicular to this magnetic field and the decay products are guided to the ends of the spectrometer through magnetic confinement. The decay volume used in these simulations is taken from the Nab proposal and is a rectangular prism with a volume of 20 x 20 x 25 mm with the longest side being in the direction of the beam. For Nab we have elected to use cylindrical coordinates $\left(\hat{r}, \hat{\phi}, \hat{z}\right)$ with the longitudinal axis of the spectrometer being the $\hat{z}$ axis of the coordinate system. The origin is chosen to be at the center of the decay volume and the $\hat{\phi}$ direction is chosen to represent right-handed rotations about the z-axis.

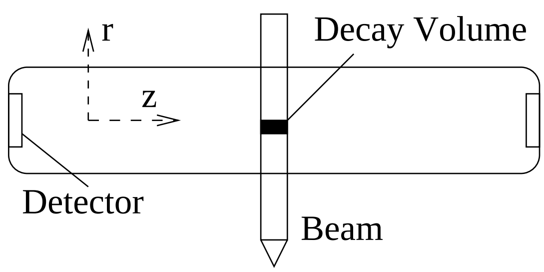

Figure 1: This figure is a schematic of Nab Experiment (Not to Scale). When the experiment is installed at the FNPB the $\hat{z}$ axis will be vertical.

Upon arriving at the end of the cavity the decay products will impinge on circular segmented silicon barrier detectors. The magnetic field will be peaked in the decay volume and rapidly fall to a low value of the same cardinality to tip the decay product's momentum along the longitudinal axis. However economic constraints restrict the size of the detectors so the magnetic field must grow near the detector to constrain the decay products to the size of the detector. Furthermore the decay protons are of such low energy that a 30 kV electric potential will be used to boost the proton's energy to the detectable range.

Having established the general features of the spectrometer the Nab collaboration selected Geant4 Monte Carlo analysis to determine the precise features of the EM field. This task includes the shape of the central peak in the magnetic field, the shape of the detector pinch in the magnetic field, and the position of the electric field near the detector.

2. Figure of Merit

In order to compare different field configurations a quantitative bench mark must be set. In our case the goal for a is to extract the proton momentum spectrum from the time of flight measurements.

2.1. Proton Momentum Response

In an ideal spectrometer all decay protons with the same momentum would register the same time of flight. This condition would result in a proton momentum spectrum of a Dirac-δ function. Our spectrometer will smear this delta function, therefore our goal is to minimize this smearing (see Figure 2). Simulating protons of a single momentum and observing the resulting smearing from our EM field we can deduce what field configuration is most effective. The FOM selected is the RMS/mean for the peak in the momentum spectrum.

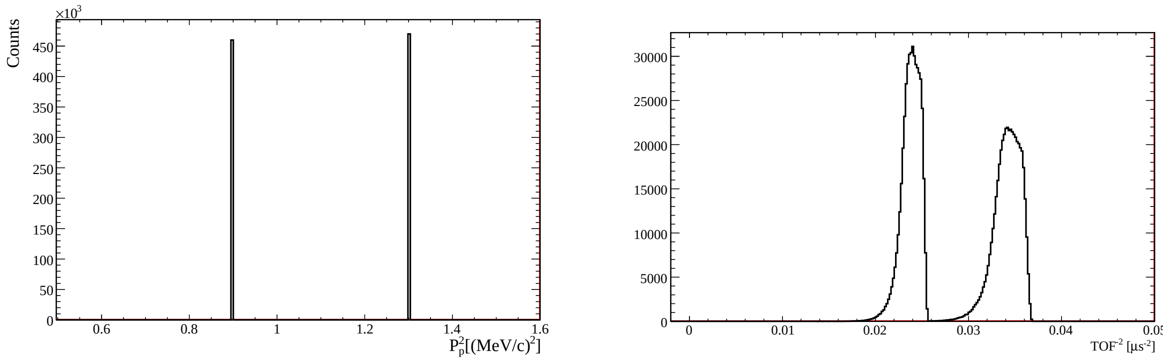

Figure 2: Left (Right): Ideal (Realistic) response for $|P_p|$ of 0.949 and 1.14 MeV/c.

2.2. Extracting a

Careful inspection of the decay rate (1) reveals that for a fixed electron energy the proton momentum spectrum is linear and the slope is proportional to a. By measuring the electron energy accurately we can then bin the proton time of flight spectrum accordingly to produce Figure 3.

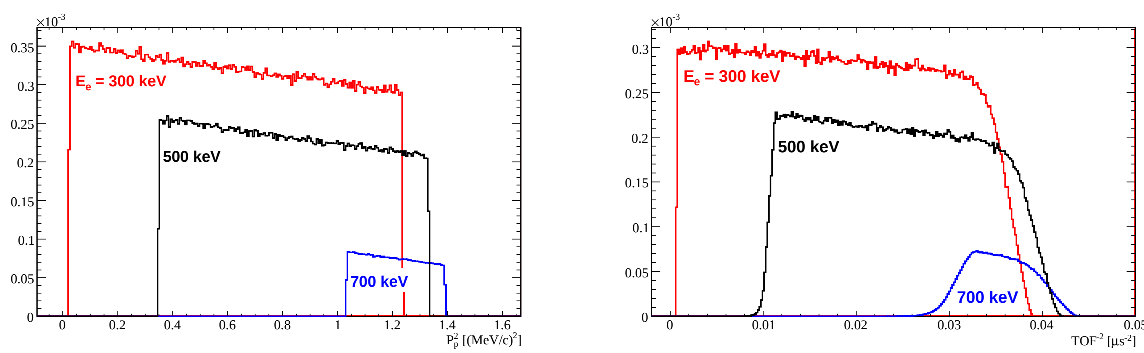

Figure 3: Left (Right): Ideal (Realistic) Spectrometer response for selected electron energies.

Fitting the simulated data we can extract the value of a. Comparing the calculation of a for different field configurations yields another way to assess which configuration is superior.

2.3. Figure of Merit for b

The determination of b comes from the electron energy spectrum in the detector. Since the detector measures the electron energy directly the form of the magnetic field plays no role in the determination of b. The only thing that must be taken into account is the 30 kV potential. The potential does provide a low energy cutoff on the electron spectrum but does not influence the shape of the spectrum. Therefore our figure of merit should be based solely on our ability to extract a.

3. Field Configurations

The studies of the EM field for Nab consists of two pieces, the central peak, and the detector pinch (Figure 4). The initial study with field map interpolation was limited in scope because we only had two EM field maps. We then increased the capability of the simulation to use an analytic function (2) for the EM field.

$$\vec{B}_{apprx} = B_0(z)\hat{z} - \frac{r}{2}\frac{\partial B_0}{\partial z}\hat{r} - \frac{r^2}{4}\frac{\partial^2 B_0}{\partial z^2}\hat{z} + \frac{r^3}{16}\frac{\partial^3 B_0}{\partial z^3}\hat{r} + \cdots \tag{2}$$

After determining what features the EM field should possesses we expanded the simulation to calculate the EM field from an arbitrary set of magnetic coils. By simulating with an arbitrary set of coils we can come to an understanding of what is practicable in real life. This calculation method was brought to the collaboration by S. Baessler and is referred to as the Ferenc method.

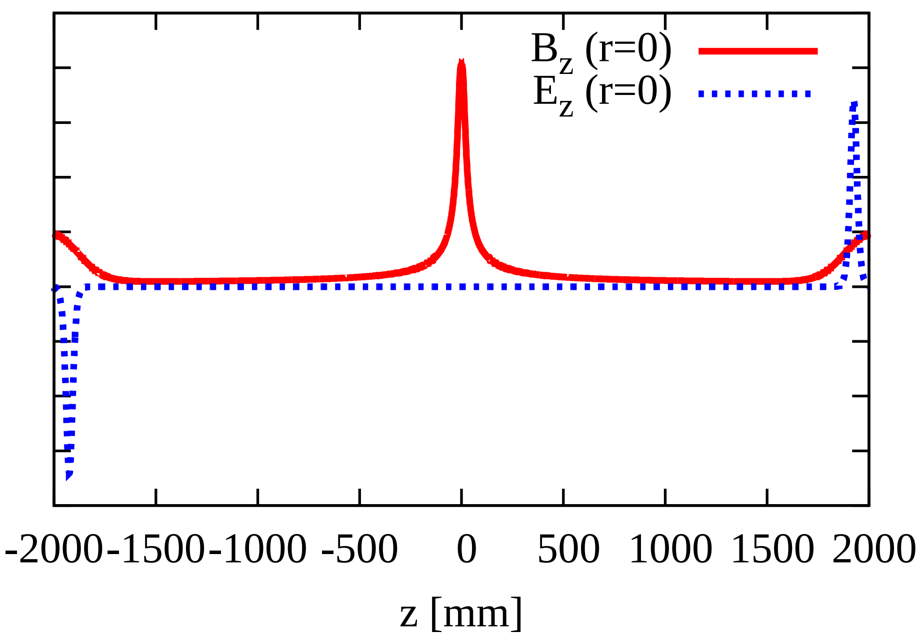

Figure 4: Qualitative example of Nab EM field

3.1. Tangent Field Simulations

The purpose of the central peak is to tip the momentum of the neutron decay products towards the $\hat{z}$ direction. If the field falls off too quickly the particles will not spend enough time in a region with a changing magnetic field, leading to incomplete longitudinalization. If the field falls off too slowly then the particle's momentum will be longitudinalized over a larger distance. This situation means a longer flight path and worse systematics. We simulated fields with a peak function of a Gaussian divided by a quadratic as well as an arc-tangent divided by a linear function. These preliminary simulations demonstrated that the arc-tangent function produced a better FOM so we the proceeded with detailed studies of the arc-tangent function parametrized as follows:

$$B_z = N \frac{\arctan\left[\beta z\left(1+\left(\frac{\beta^2}{3}-\alpha^2\right)z^2\right)\right]}{\beta z} + \epsilon. \quad (3)$$

In this parametrization α represents the curvature of the field at the origin and β represents the adiabaticity of the field (larger β means less adiabatic). In order to keep the simulation as simple as possible the first two terms of (2) were used. Figure 5 and Figure 6 show results for various α and β. Figure 7 and Figure 8 show detailed results for selected α and β.

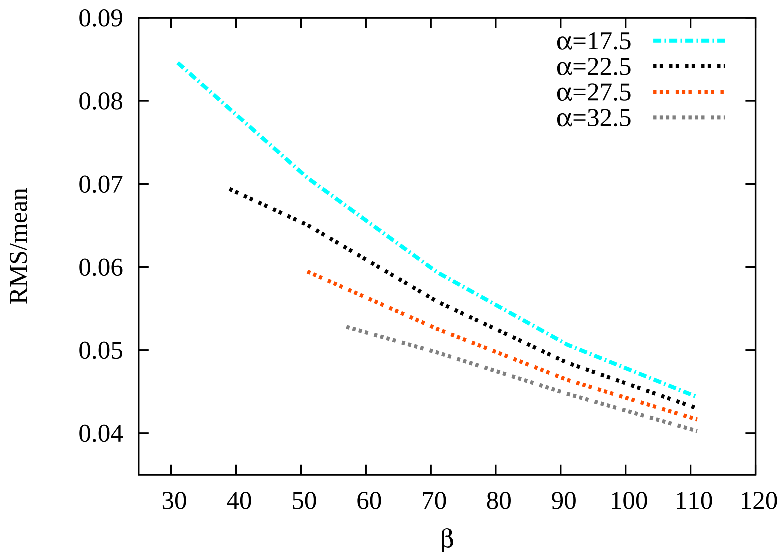

Figure 5: Figure of Merit for various α and β

3.2. Ferenc Method Simulations

Having learned about the behavior of fields with the tangent method we moved on to simulating magnetic coils with the Ferenc method. Immediately we found that the data exhibits a tail in the $1/TOF^2$ spectrum that wasn't present in the tangent simulations (compare Figure 8 with Figure 9). The events in this tail are the events which have a large radius of the decay point. We applied a cut of 5 mm for the maximum radius for the decay point and then the tail vanishes (Figure 10). In order to quantify the size of the tail we also look at the 10^{-4} quantile of the TOF (Figure 6).

Currently we are producing new coil configurations and running simulations. Figures 11-22 (at the end of the document) show the results thus far.

Since the completion of this document advances have been made in the simulation. The decay volume has been redefined to be a cylinder with the same orientation as the spectrometer. Also the coil configurations have been modified to make physical sense. These upgrades allowed us to test the designed decay volume for the different coils. Figure 14 shows the results for the upgraded simulation for our best set of coils.

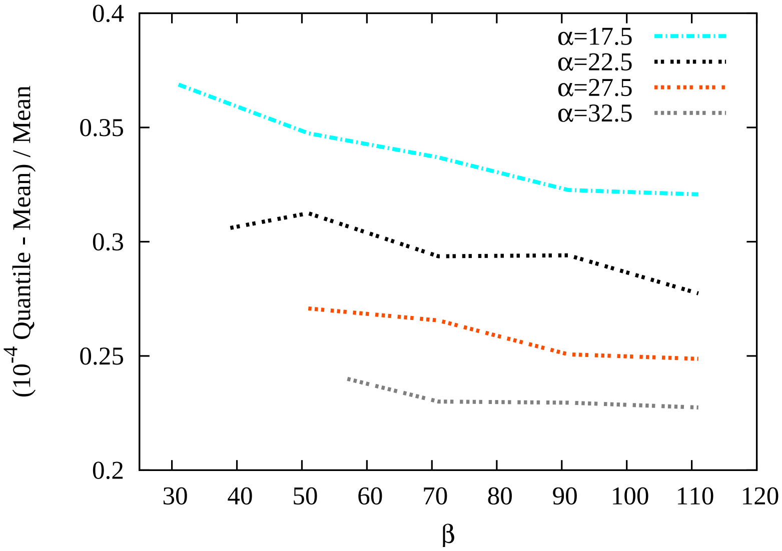

Figure 6: Figure of Merit 10^{-4} Quantile for various α and β

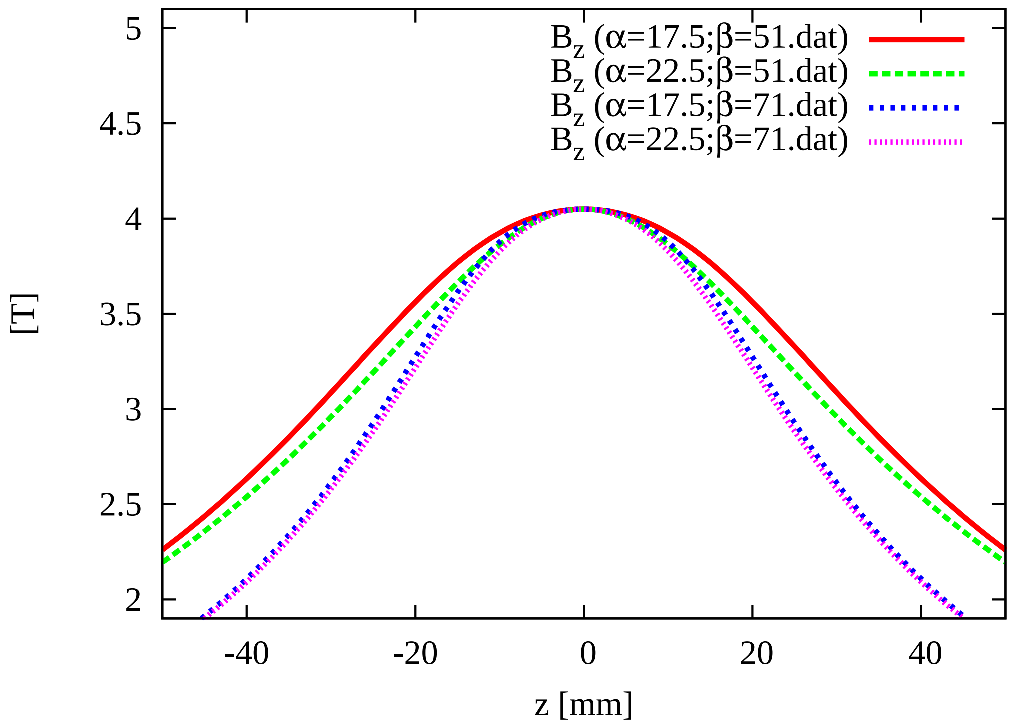

Figure 7: Field profiles near the decay region

4. The Hardware

The Galileo cluster operated by the Physics Department of the University of Virginia consists of 36 nodes. Of these nodes 30 are configured for batch operation and 6 for user login purposes. This cluster is open to the UVa community but is principally used by a few graduate students from the physics department. Each node possesses 2 CPUs and each CPU is hyperthreaded. Nominally

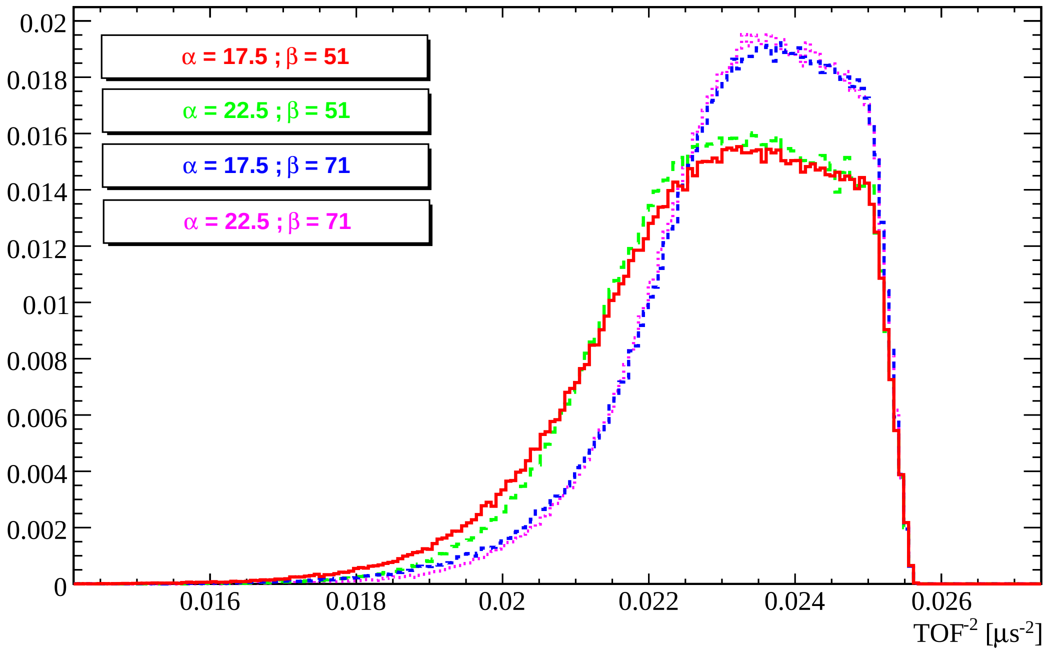

Figure 8: Detector response for protons with $|P_p| = 0.949\,\mathrm{MeV/c}$ for selected fields

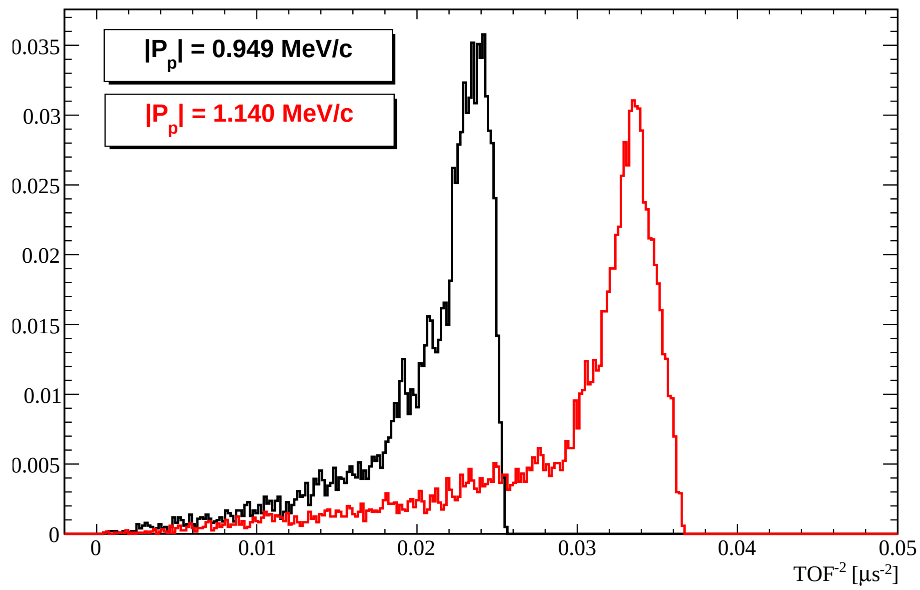

Figure 9: Ferenc method detector response for full decay volume.

the user sees each node possessing 4 processors and each processor operates at 3 Ghz. Each node has 4 Gb of RAM. Of the 30 batch nodes 10 are owned by the Počanić group and therefore jobs submitted by users from that group receive top priority on those nodes. In effect this means that, at any time, the group may submit 40 jobs and they will run to completion without delay. This management is done by Condor. Finally, all of Galileo is linked with a 1 Gb ethernet network.

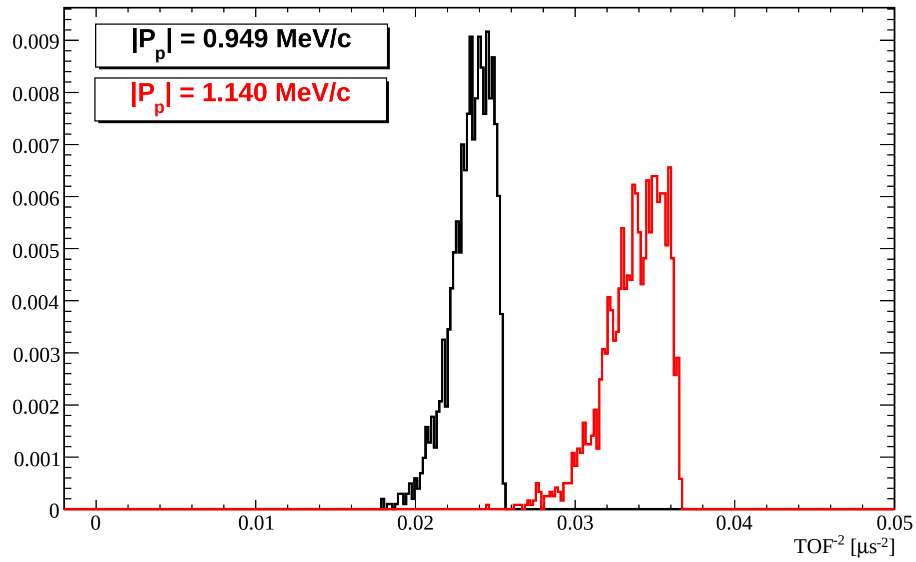

Figure 10: Ferenc method detector response for maximum decay radius 5 mm.

5. The Software

The Nab Monte Carlo simulations on Galileo are run on different versions of Geant4 with the version being determined by the user. The user lpa2a employs Geant4.9.0 with CLHEP library package 2.0.3.1. Source code downloads for this software is available at the CERN website, `http://geant4.web.cern.ch/geant4/support/source_archive.shtml`. The data analysis package employed is Root version 5.14/00e. Both Geant4 and Root are object oriented C++ programs produced by a collaboration at CERN.

6. Geant4 Specifics

The Geant creators recommend that all users take an example project and modify it to their needs. For the Nab simulations we have modified Geant example TestEm5. The spectrometer geometry is a volume that contains two silicon cylinders spaced 4 m apart. The volume can be configured to contain a gas at a given pressure (i.e. 10^{-8} torr). Also a class based on FermiLab beam tools was created to manage the EM field of the spectrometer. This class can accommodate a field map, an analytic function, or a set of fictitious coils. After lengthy study we selected G4CashkarpRKF45 for our integration stepper. The parameters for this stepper have been chosen to produce an accuracy in the time of flight of typical Nab events to be on the order of picoseconds. The random engine used for these simulations is the Geant4 built in generator called with the method G4UniformRand().

PhysList is not a method, rather in the physics list for a particle one must add the G4StepLimiter process for tracking particles through a vacuum. If this process is not added then the particle will jump over the vacuum region in one step (this behavior varies from version to version). G4UserLimits is called from a pointer to a logical volume in the Detector Construction method ConstructCalorimieter. In the DetectorConstruction method SetMagField, SetMinimumepsilonStep, SetMaximumEpsilonStep, and SetDeltaOneStep are called via a pointer to the field manager. G4MagInt_Driver is constructed after the integration stepper is constructed but before the chord finder is constructed. For this simulation these constructions take place in SetMagField after the emField and managers are constructed.

Method	Value
PhysList	AddProcess(new G4StepLimiter,-1,-1,3)
G4UserLimits()	uekinMin = 0.
G4UserLimits()	urangMin = 0.
G4UserLimits()	utimeMax = 1.E-3*s
G4UserLimits()	ustepMax = 1.0*mm
G4UserLimits()	utrakMax = 4.010*m
G4FieldManager()	DeltaChord = 1.E-5*mm
G4FieldManager()	DeltaOneStep = 1.E-12*mm
G4FieldManager()	MinimumEpsilonStep = 1.E-12
G4FieldManager()	MaximumEpsilonStep = 1.E-12
G4MagInt_Driver()	nvar = 8
G4MagInt_Driver()	hmin = 0.001*mm
G4MagInt_Driver()	G4CashKarpRKF45(emEquation,nvar)

Table 1: Summary of Edited Geant4 Settings

References

1. J.D. Jackson, S.B. Treiman, and Jr. H.W. Wyld. Possible tests of time reversal invariance in beta decay. *Physical Review*, 106:517, 1957.

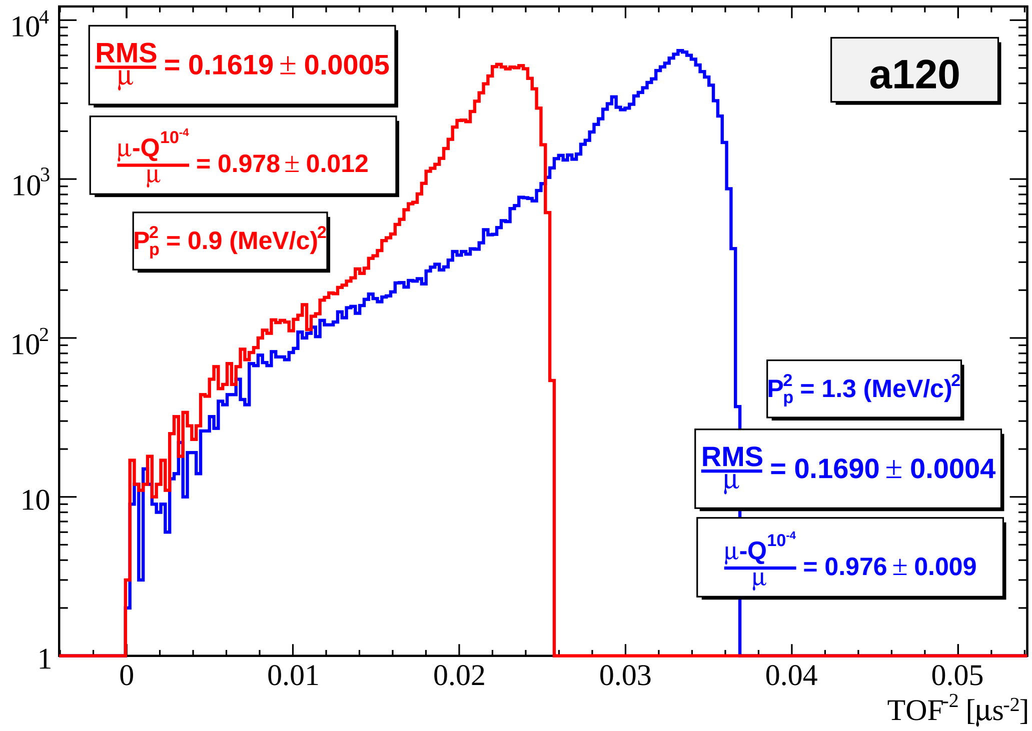

Figure 11: Ferenc method detector response for coils a120 (see Figure 18).

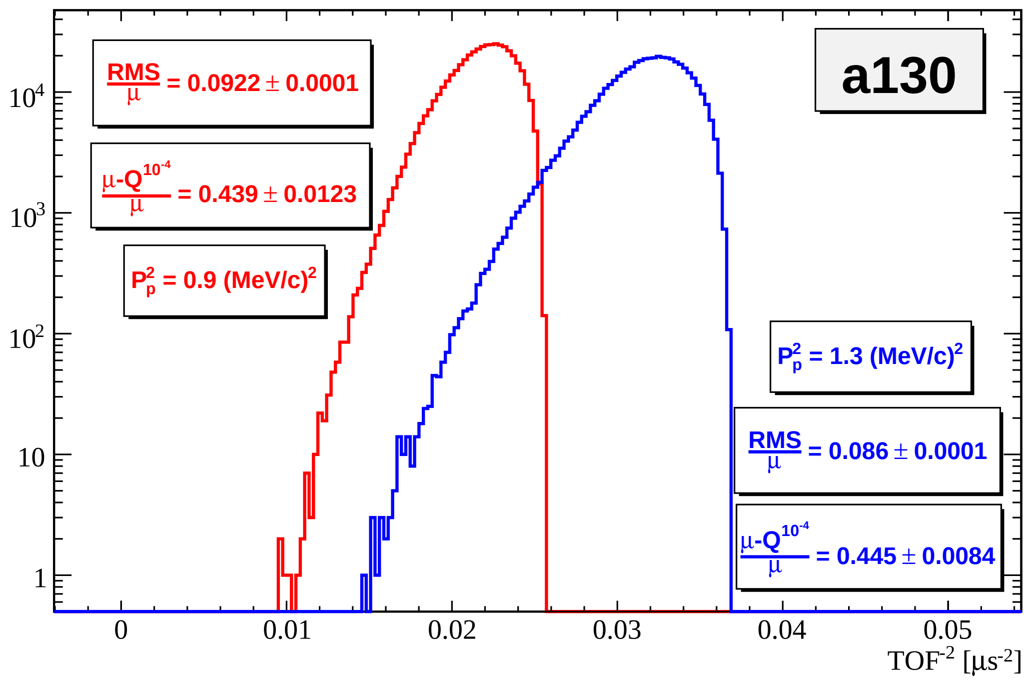

Figure 12: Ferenc method detector response for coils a130 (see Figure 19).

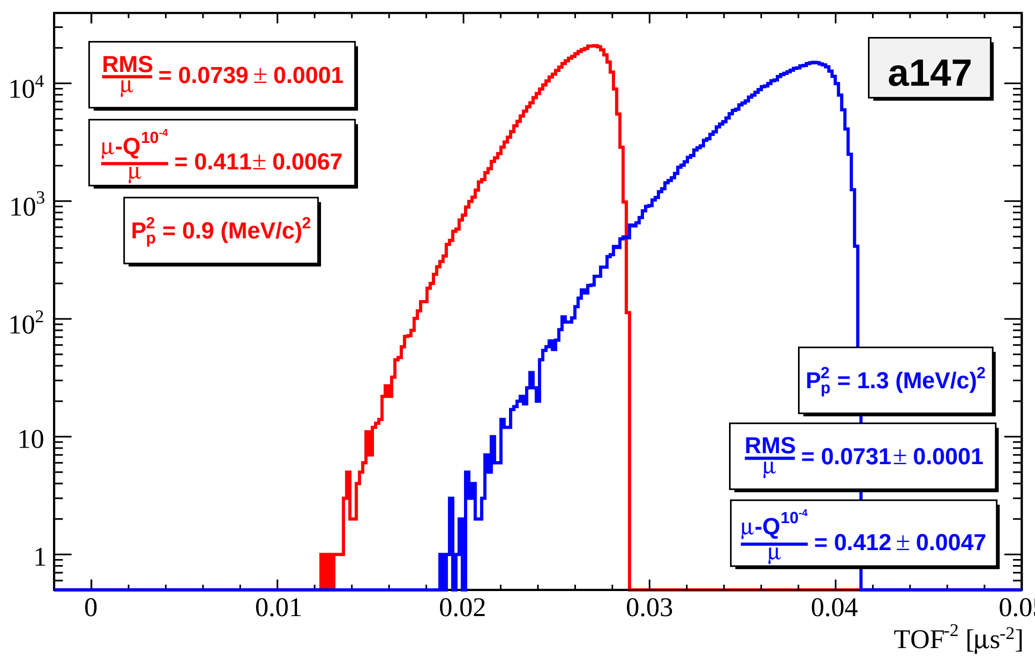

Figure 13: Ferenc method detector response for coils a147 (see Figure 20).

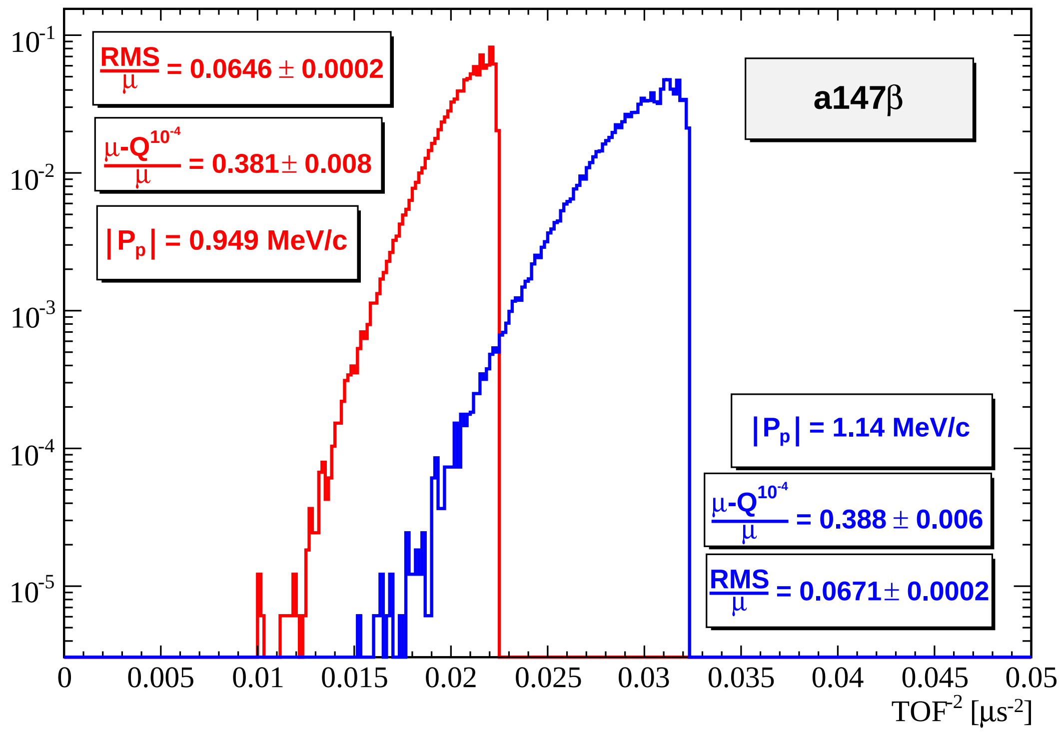

Figure 14: Coil configuration a147beta

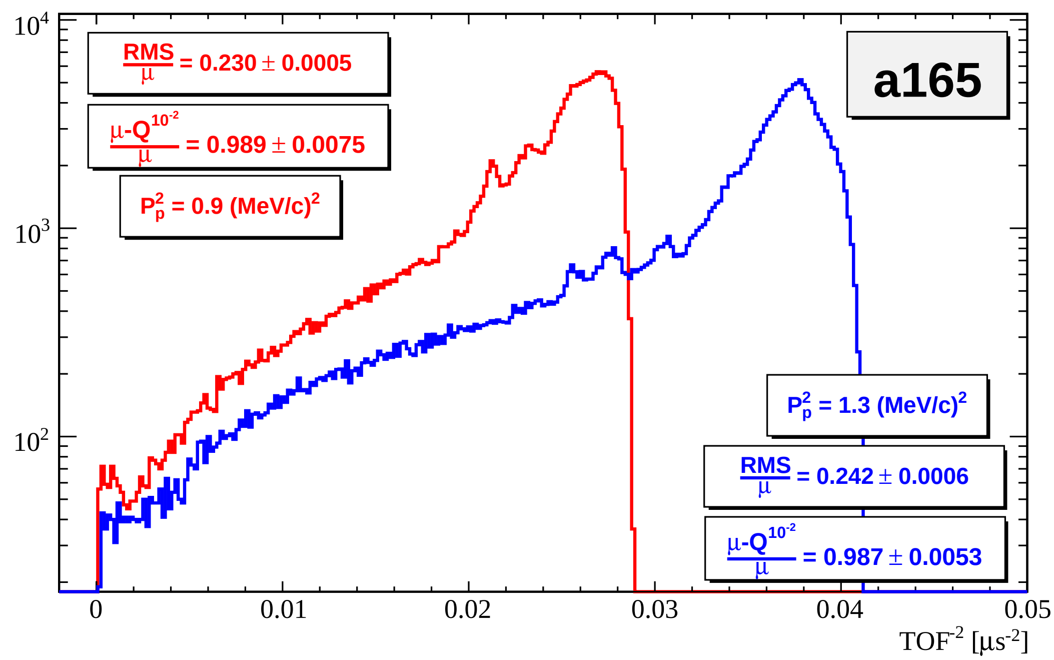

Figure 15: Ferenc method detector response for coils a165 (see Figure 21).

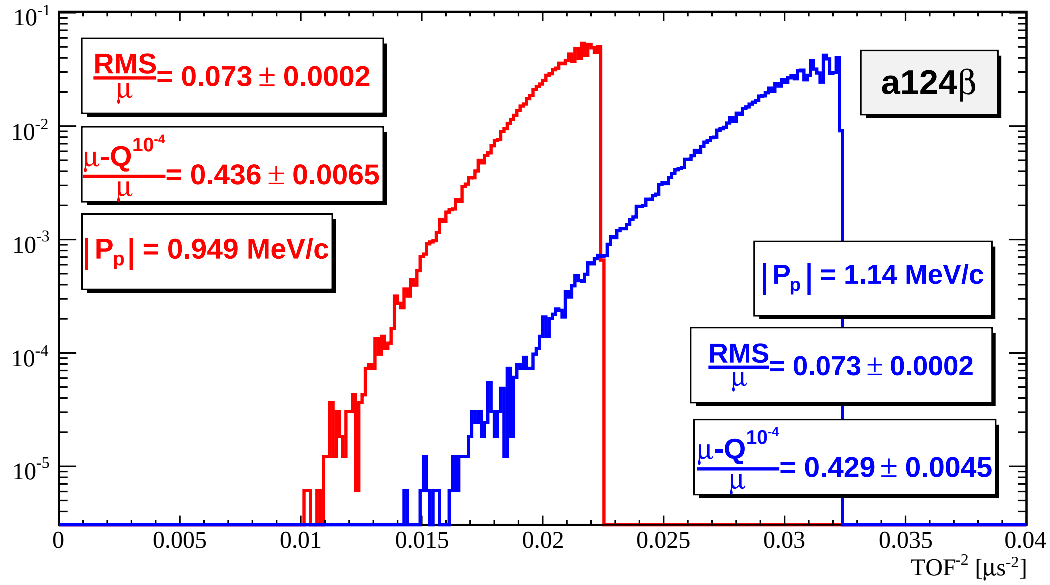

Figure 16: Coil configuration a124beta

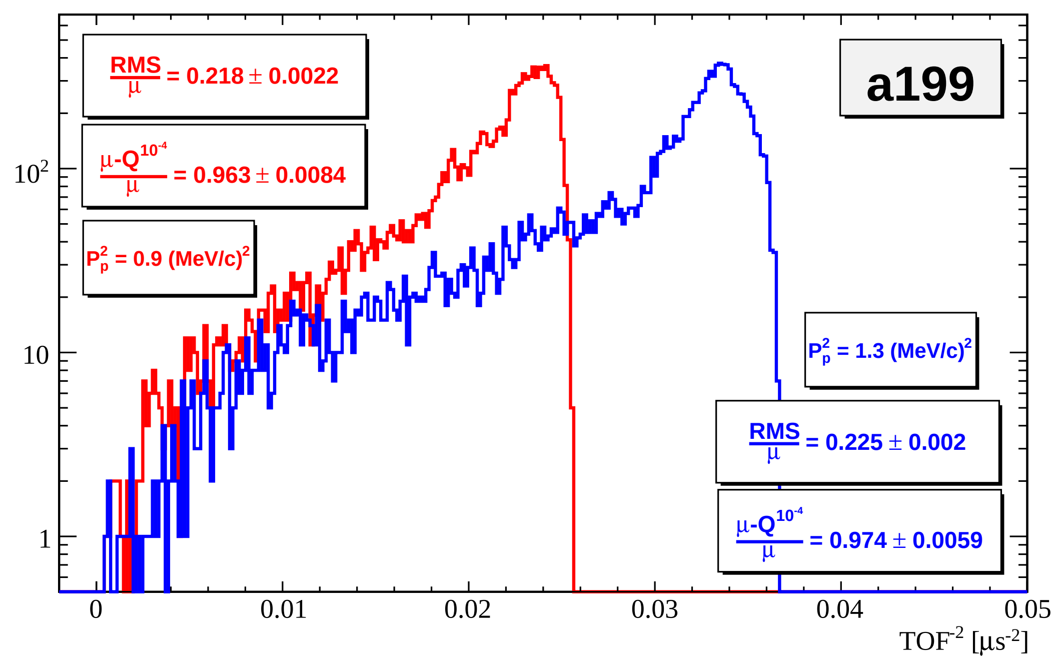

Figure 17: Ferenc method detector response for coils a199 (see Figure 22).

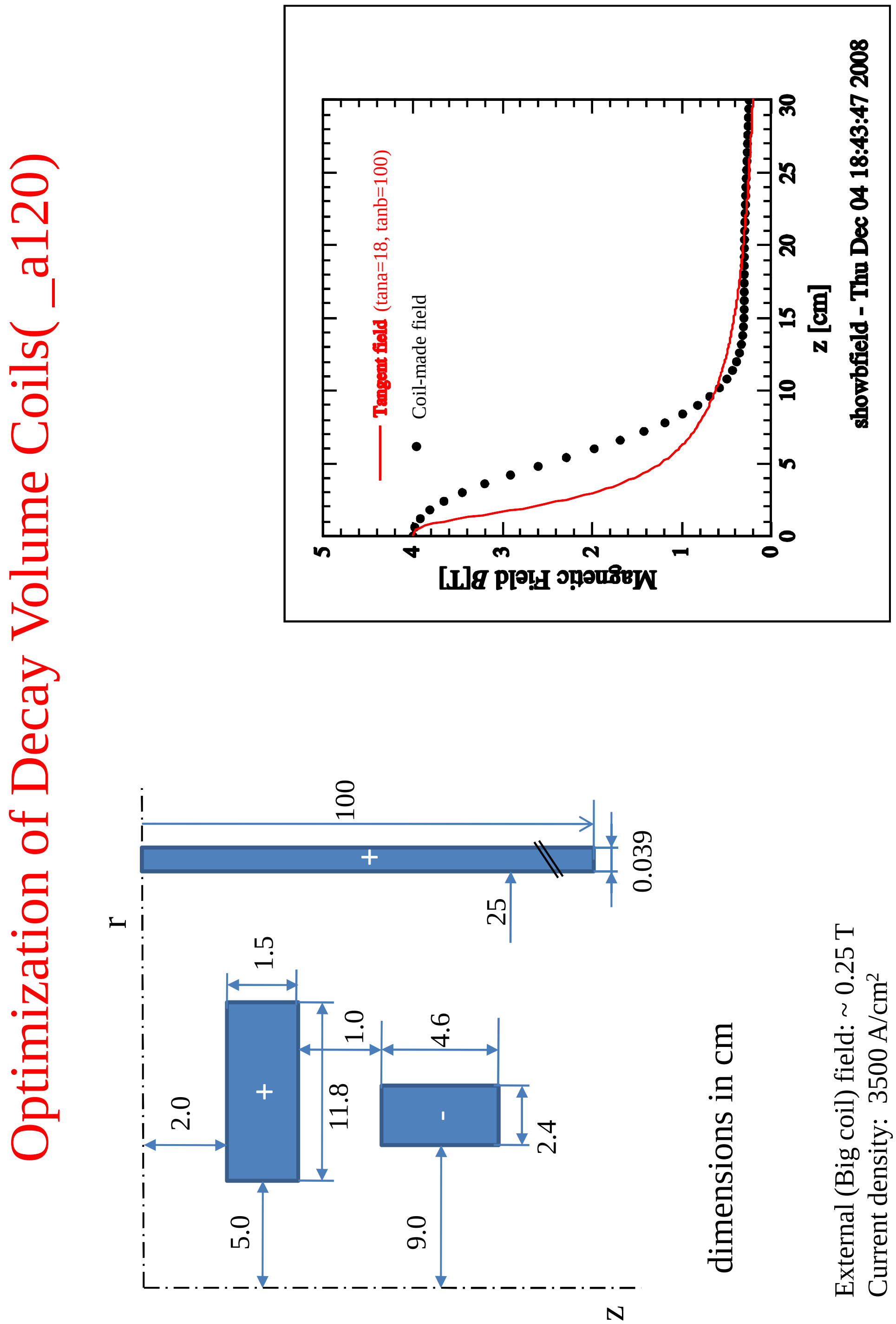

Figure 18: Coil configuration a120

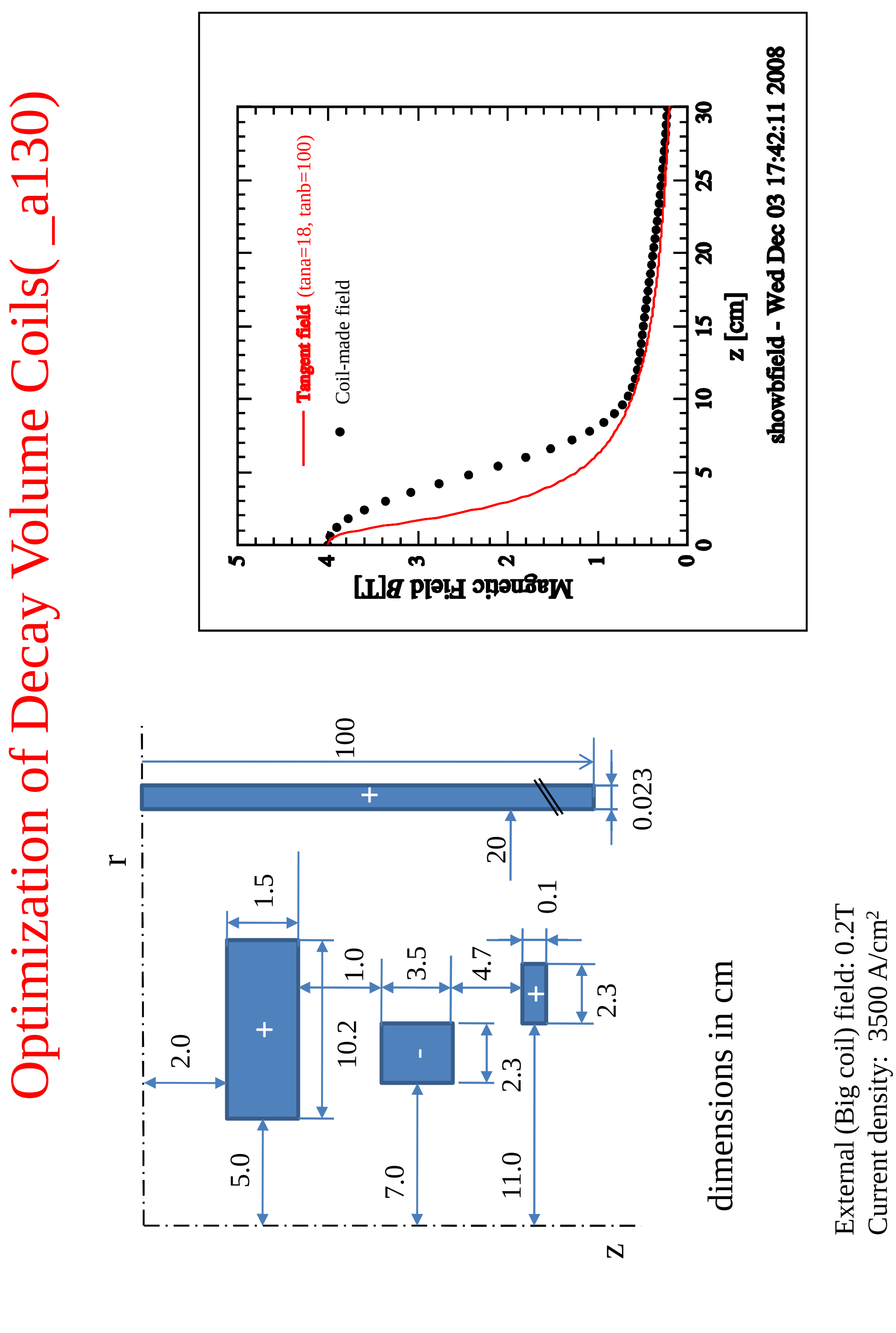

Figure 19: Coil configuration a130

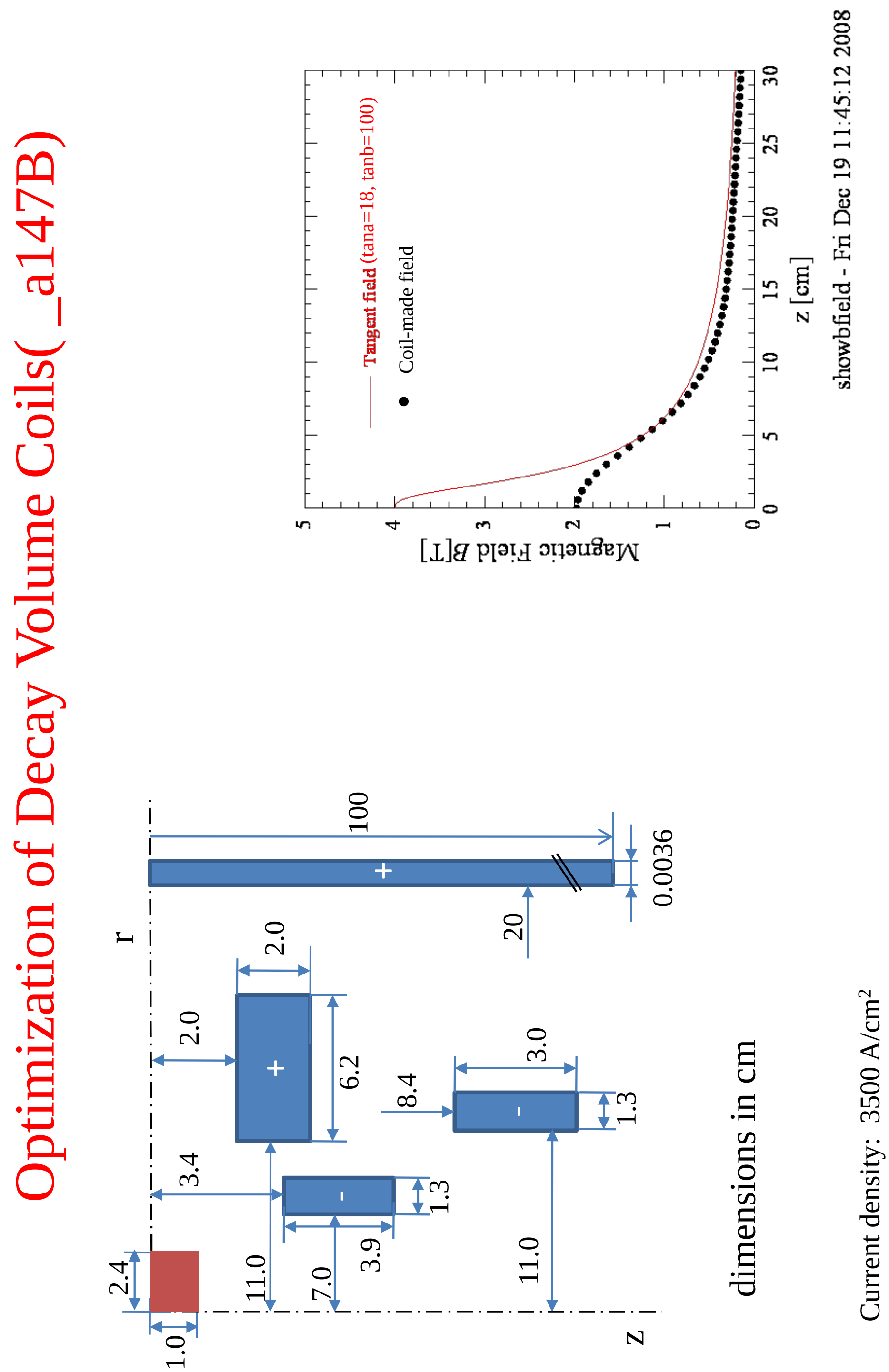

Figure 20: Coil configuration a147

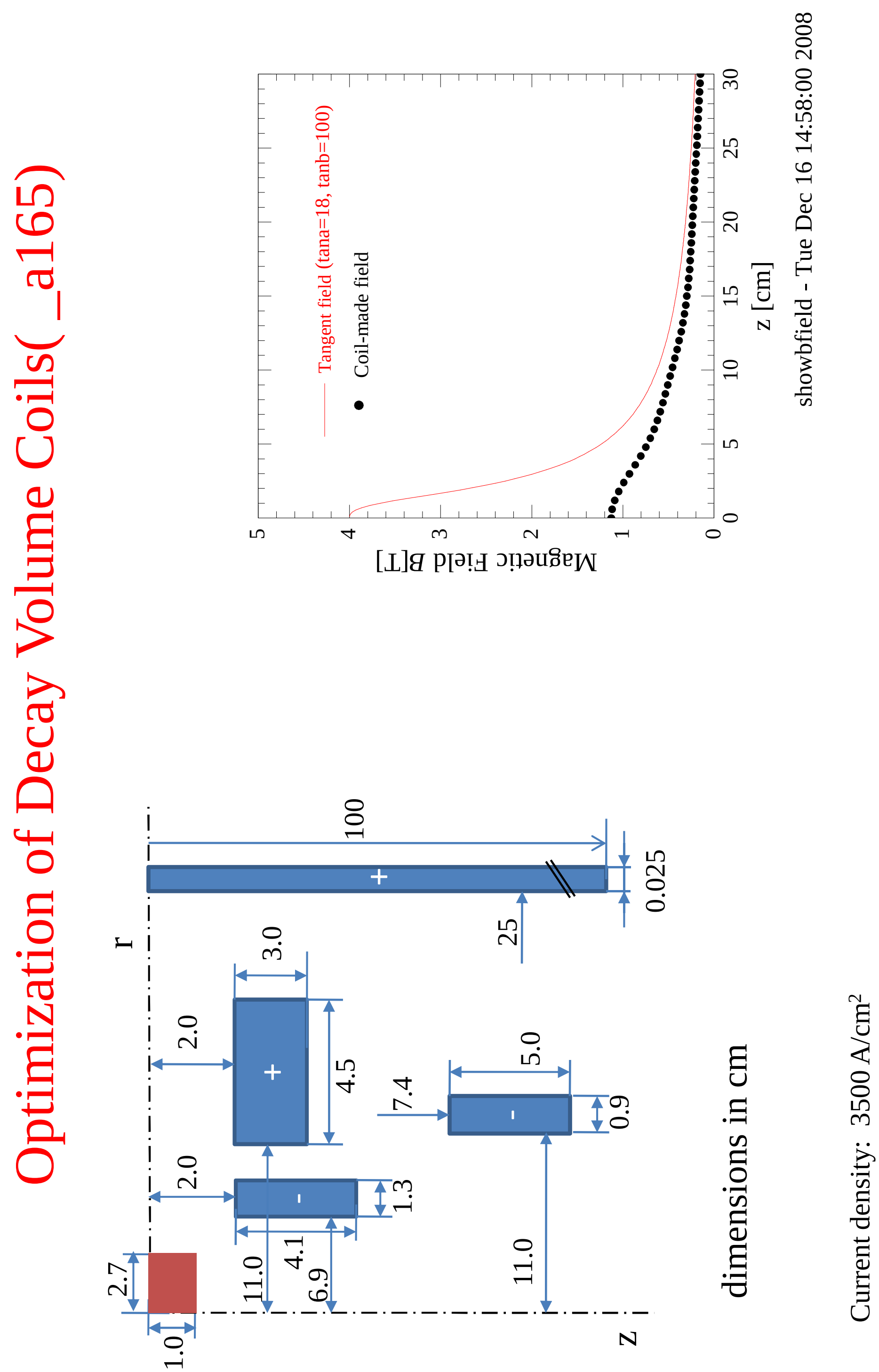

Figure 21: Coil configuration a165

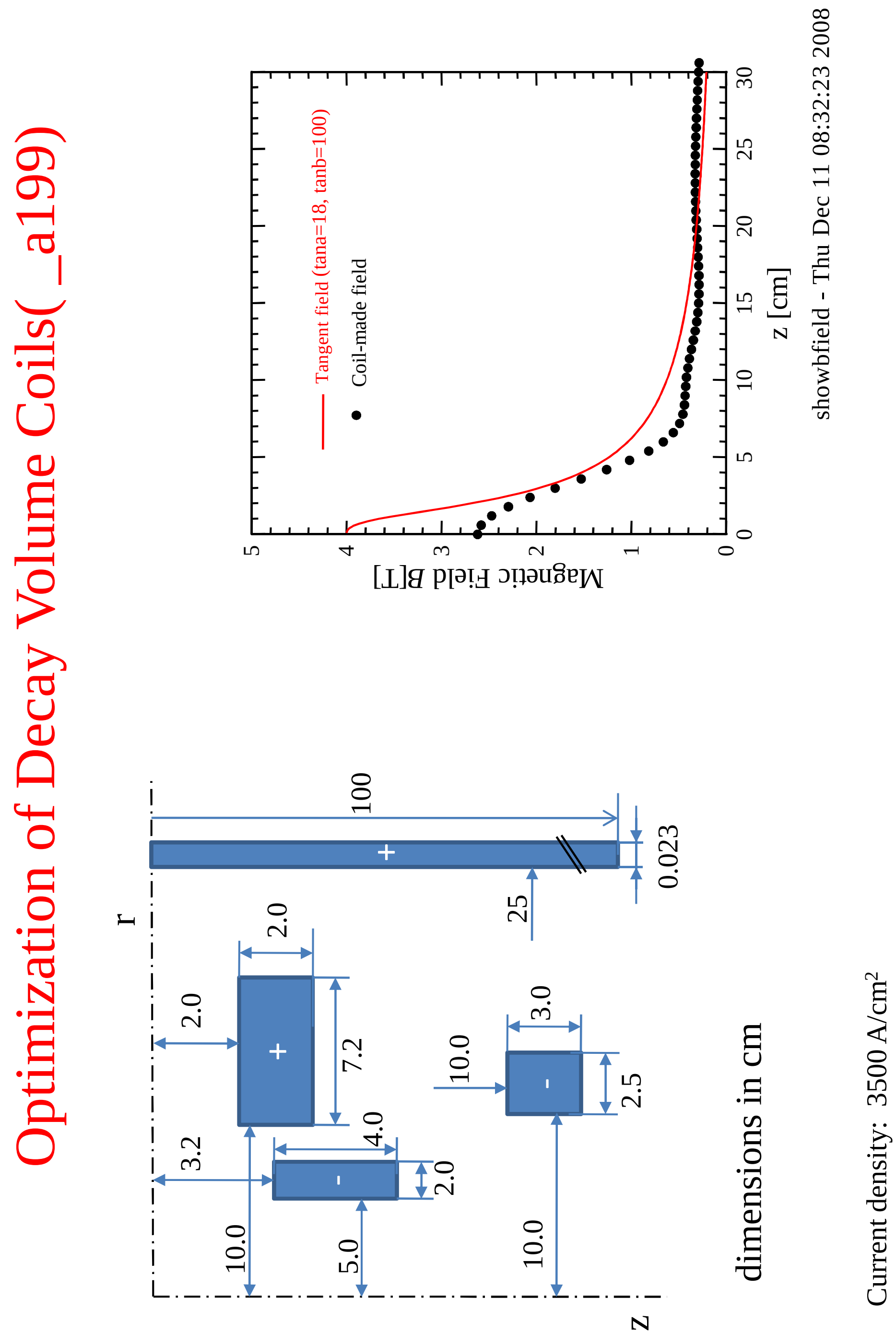

Figure 22: Coil configuration a199

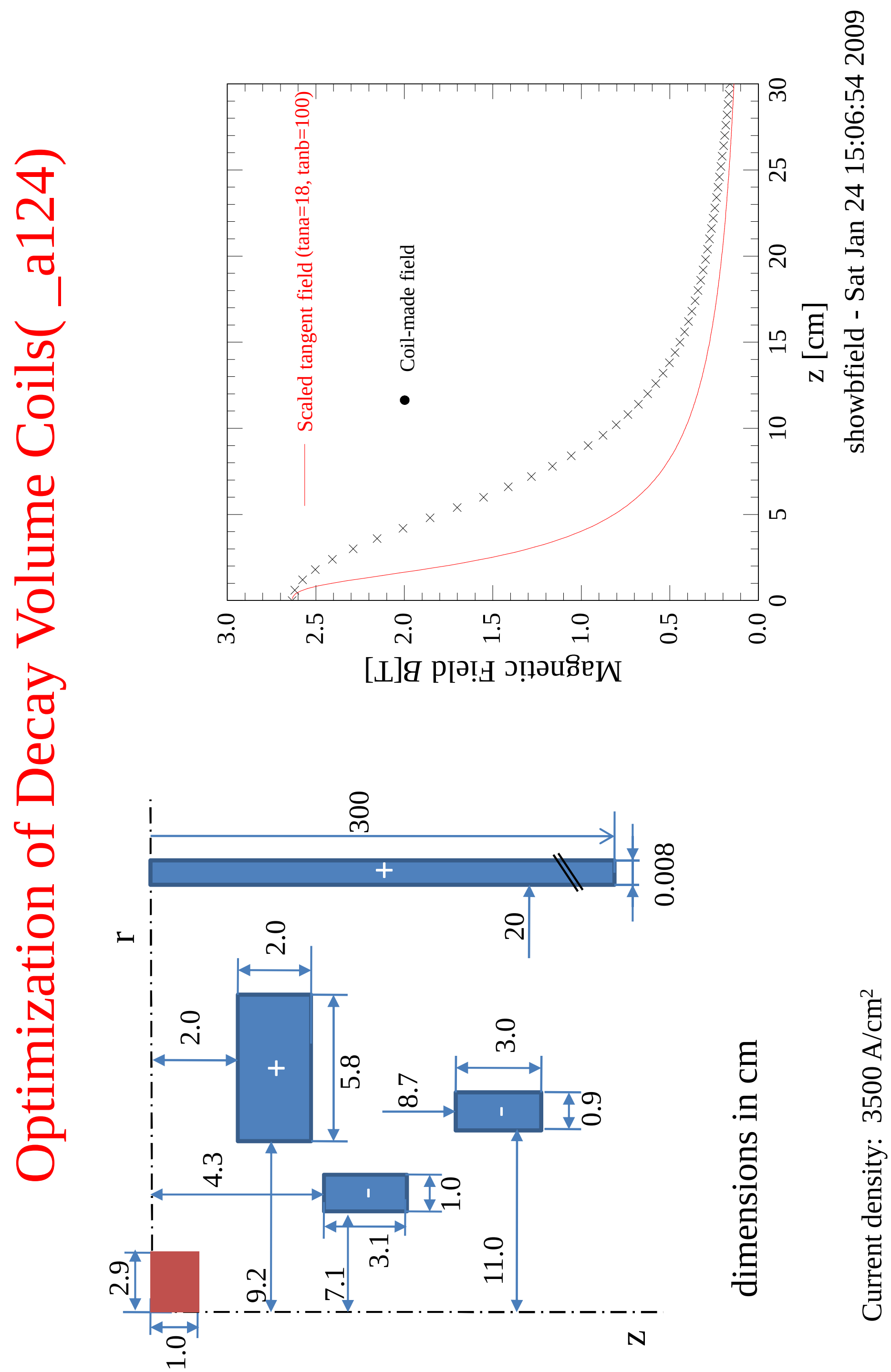

Figure 23: Coil configuration a124